Synthesis and Electrochemical and Theoretical Studies of Fischer-Type Alkenyl−Carbyne Tungsten Complexes $[(dppe)(CO)_2(RNC)W\{\equiv CCH{=}C\overline{CH_2CH_2(CH_2)_nCH_2}\}][BF_4]$ (R = Alkyl, Aryl)†

Lei Zhang,‡ M. Fátima C. Guedes da Silva,‡,⊥ Maxim L. Kuznetsov,‡ M. Pilar Gamasa,§ José Gimeno,*,§ João J. R. Fraústo da Silva,‡ and Armando J. L. Pombeiro*,‡

Centro de Química Estrutural, Complexo I, Instituto Superior Técnico, Av. Rovisco Pais, 1049-001 Lisbon, Portugal, Instituto Universitario de Química Organometálica "Enrique Moles" (Unidad Asociada al CSIC), Departamento de Química Orgánica e Inorgánica, Facultad de Química, Universidad de Oviedo, 33071 Oviedo, Spain, and Universidade Lusófona de Humanidades e Tecnologias, Av. Campo Grande 376, 1749-024 Lisbon, Portugal

Received December 28, 2000

The cationic isocyanide alkenyl-carbyne complexes *cis*-$[(dppe)(CO)_2(RNC)W\{\equiv C{-}CH{=}\overline{CCH_2CH_2(CH_2)_nCH_2}\}][BF_4]$ [dppe = κ^2-(*P*,*P*)-$Ph_2P(CH_2)_2PPh_2$; R = Bu^n, *n* = 1 (**2a**); R = Bu^t, *n* = 1 (**2b**), 4 (**2c**); R = Cy, *n* = 1 (**2d**), 4 (**2e**); R = $PhCH_2$, *n* = 1 (**2f**), 4 (**2g**); R = 2,6-$Me_2C_6H_3$, *n* = 1 (**2h**), 4 (**2i**)] were prepared by reactions of the corresponding acetonitrile complexes *trans*-$[(dppe)(CO)_2(NCMe)W\{\equiv C{-}CH{=}\overline{CCH_2CH_2(CH_2)_nCH_2}\}][BF_4]$ [*n* = 1 (**1a**), 4 (**1b**)] with the appropriate isocyanide. Ab initio quantum-chemical methods at the RHF and single-point MP2 levels of theory were applied to the investigation of the structure, bonding, oxidation potential, and relative isomeric stability at the model complexes *trans*- and *cis*-$[(PH_3)_2(CO)_2(L)W(\equiv C{-}CH{=}CH_2)]^{m+}$ [L = Cl^- (*m* = 0), NCMe (*m* = 1), CNMe (*m* = 1), or CO (*m* = 1)], which also comprise the related carbonyl and chloride species, allowing a comparison of the effects of the Cl^-, NCMe, CNMe, and CO ligands, which are shown to follow their electron π-donor/acceptor properties. The electrochemical behavior of complexes **2a**−**i**, as well as that of the related carbonyl, phosphine $[(dppe)(CO)_2(L)W\{\equiv C{-}CH{=}\overline{CCH_2CH_2(CH_2)_nCH_2}\}][BF_4]$ [L = CO; *n* = 1 (**3a**), 4 (**3b**); L = PMe_3, *n* = 1 (**4a**)] and phosphinodithiocarboxylate $[(dppe)(\kappa^3\text{-}S_2CPCy_3)W\{\equiv C{-}CH{=}\overline{CCH_2CH_2(CH_2)_nCH_2}\}][BF_4]$ [*n* = 1 (**5a**), 4 (**5b**)] compounds, was investigated by cyclic voltammetry and controlled potential electrolysis in aprotic media and at a Pt electrode. The oxidation potential follows the order of the net π-electron acceptor minus σ-donor character of the ligands, and from the observed linear dependence on the electrochemical P_L ligand parameter it was possible to estimate the values of the electron-richness (E_S) and polarizability (β) parameters for the binding metal fragments containing alkenyl-carbyne ligands, $\{(dppe)(CO)_2W(\equiv C{-}CH{=}\overline{CCH_2CH_2(CH_2)_nCH_2}\}^+$, indicating they exhibit rather low electron-richness and polarizability, which are accounted for by the very strong π-electron acceptance of the coordinated alkenyl-carbyne groups. These ligands are activated toward proton loss by anodic oxidation of their complexes.

Introduction

Unsaturated alkylidyne metal derivatives belong to the well-known series of Fischer-type carbyne transition metal complexes.[1] However only a rather limited number of examples have been described to date.[2] We have recently reported[2h−k] a series of this class of derivatives in which α,β-cycloalkenyl carbyne groups are bound to tungsten carbonyl fragments in an octahedral geometry (type **A**; Scheme 1). The systematic presence of *trans* monodentate ligands with respect to the carbyne group contrasts with the precursor tricarbonyl species (type **B**; Scheme 1) where the π-acceptor carbonyl group occupies *cis* coordination sites. Actually complexes **A** (L = halides, MeCN) are obtained from **B** (L = CO) through an exchange reaction of the ligands via an isomerization process.[2h]

It is apparent that the π-electronic properties of both the unsaturated carbyne group and the entering ligand

† Dedicated to Professor Rafael Usón on the occasion of his 75th birthday.

‡ Instituto Superior Técnico, fax: +351-218464455, e-mail: pombeiro@ist.utl.pt.
§ Universidad de Oviedo, fax: +34-985103446, e-mail: jgh@sauron.quimica.uniovi.es.
⊥ Universidade Lusófona de Humanidades e Tecnologias.

10.1021/om001095g CCC: $20.00
Publication on Web 05/25/2001

Scheme 1. Alkenyl-Carbyne Complexes: A (*trans*) and B (*cis*)

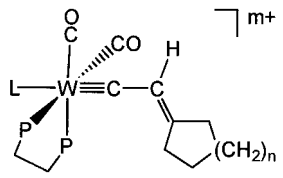

A

m=0; L= F, Cl, Br, I, CN, SCN, OCN.
m=1; L= MeCN, PMe_3.

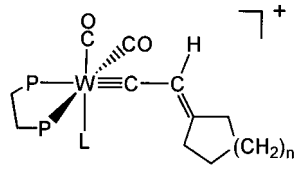

B

govern the stereochemistry of the resulting complex. This prompted us to study the scope of this behavior, including MO calculations, within our interest[2i,3,4] on the application of theoretical calculations to the interpretation of the chemical and electrochemical behaviors of complexes with multiple metal−carbon bonds. In contrast to the well-developed experimental chemistry of carbyne complexes,[1] only a rather limited number of theoretical studies on this type of complexes have been reported,[2i,3,5−11] in some cases involving only EHMO calculations, and they have been commonly devoted mainly to the understanding of the metal−carbon triple bond. Moreover, electrochemical studies on carbyne complexes are also rather scarce,[1b,2j,12−17] despite their interest for the understanding of the electron donor/acceptor properties of the carbyne ligands and for the activation of the complexes toward further reactions upon electron transfer.

In this paper we now report (a) the synthesis and electrochemical studies of novel cationic isocyanide derivatives of the type **B** [P−P = dppe; L = CNR: R = Bu^n; n = 4 (**2a**); R = Bu^t; n = 1 (**2b**), 4 (**2c**); R = Cy; n = 1 (**2d**), 4 (**2e**); R = $PhCH_2$; n = 1 (**2f**), 4 (**2g**); R = 2,6-$Me_2C_6H_3$; n = 1 (**2h**), n = 4 (**2i**)] (Scheme 2), (b) ab initio theoretical studies directed to rationalize the oxidation potentials of this type of derivatives, and (c) structure and bonding analyses through ab initio calculations for (i) both *trans* and the experimentally found *cis* isocyanide carbyne derivatives, as well as for (ii) the related acetonitrile-, carbonyl-, and chloro-carbyne isomers, thus also allowing a comparison of the electronic effects of these ligands on the relative isomeric stabilities of the various carbyne complexes.

Results and Discussion

Synthesis and Characterization of Complexes 2a−i. The reaction of the acetonitrile complex **1a** or **1b** with an equimolar amount of the corresponding isocyanide in dichloromethane at room temperature leads to the facile substitution of acetonitrile ligand, affording the novel cationic isocyanide *cis*-dicarbonyl alkenylcarbyne complexes **2a−2i** in high yields (Scheme 2).

Elemental analyses and mass (FAB), IR, and ^1H, $^{31}P\{^1H\}$, and $^{13}C\{^1H\}$ NMR spectroscopic data (Tables 1 and 2, and the Experimental Section) support the proposed formulations. The IR spectra (CH_2Cl_2) of **2a−2i** show the typical carbonyl stretching absorptions ν(CO) in the range 2007−2009 and 1948−1955 cm^{-1} for *cis*-dicarbonyl arrangement. Furthermore, a medium-intensity band in the range 2136−2187 cm^{-1} associated with ν(CN) is also observed for all the compounds.

The formation of the complexes bearing a *cis* isocyanide−carbyne arrangement is supported by the $^{31}P\{^1H\}$ NMR spectra (Table 1) since they show two singlet resonances at δ 20.0−21.6 and 39.4−40.3, indicating the chemical inequivalence of the two phosphorus nuclei of dppe. The low-field signal with J(P−W) = 229.8−236.2 Hz is typical of the phosphine *trans* to the carbonyl ligand.[2h] The high-field signal with J(P−W) = 83.3−85.1 Hz is assigned to the phosphorus nucleus *trans* to the carbyne group, [2h] reflecting the high *trans* influence of the carbyne ligand.[18] The ^1H NMR spectra show a

(1) (a) Fischer, H.; Hofmann, P.; Kreissl, F. R.; Schrock, R. R.; Schubert, U.; Weiss, K. In *Carbyne Complexes*; VCH: New York, 1988. (b) *Transition Metal Carbyne Complexes*; Kreissl, F. R., Ed.; NATO ASI Series; Kluwer Academic: Dorderecht, The Netherlands, 1993. (c) Mayr, A.; Hoffmeister, H. *Adv. Organomet. Chem.* **1991**, *32*, 227.

(2) For recent developments see: (a) Woodworth, B. E.; White, P. S.; Templeton, J. L. *J. Am. Chem. Soc.* **1997**, *119*, 828, and references therein. (b) Main, D. E.; McElwee-White, L. *J. Am. Chem. Soc.* **1997**, *119*, 4551. (c) Woodworth, B. E.; Frohnapfel, D. S.; White, P. S.; Templeton, J. L. *Organometallics* **1998**, *17*, 1655. (d) Yu, M. P. Y.; Mayr, A.; Cheung, K. K. *J. Chem. Soc., Dalton Trans.* **1998**, 475. (e) Yu, M. P. Y.; Mayr, A.; Cheung, K. K. *J. Chem. Soc., Dalton Trans.* **1998**, 2373. (f) Yu, M. P. Y.; Mayr, A. *J. Organomet. Chem.* **1999**, *577*, 223. (g) Mayr, A.; Yu, M. P. Y.; Yam, V. W.-W. *J. Am. Chem. Soc.* **1999**, *121*, 1760. (h) Zhang, L.; Gamasa, M. P.; Gimeno, J.; Carbajo, R. J.; López-Ortiz, F.; Lanfranchi, M.; Tiripicchio, A. *Organometallics* **1996**, *15*, 4274. (i) Zhang, L.; Gamasa, M. P.; Gimeno, J.; Galindo, A.; Mealli, C.; Lanfranchi, M.; Tiripicchio, A. *Organometallics* **1997**, *16*, 4099, and references therein. (j) Zhang, L.; Gamasa, M. P.; Gimeno, J.; Carbajo, R. J.; López-Ortiz, F.; Guedes da Silva, M. F. C.; Pombeiro, A. J. L. *Eur. J. Inorg. Chem.* **2000**, 341. (k) Zhang, L.; Gamasa, M. P.; Gimeno, J.; Guedes da Silva, M. F. C.; Pombeiro, A. J. L.; Graiff, C.; Lanfranchi, M.; Tiripicchio, A. *Eur. J. Inorg. Chem.* **2000**, 1707.

(3) (a) Carvalho, M. F. N. N.; Pombeiro, A. J. L.; Bakalbassis, E. G.; Tsipsis, C. A. *J. Organomet. Chem.* **1989**, *371*, C26. (b) Bakalbassis, E. G.; Tsipsis, C. A.; Pombeiro, A. J. L. *J. Organomet. Chem.* **1991**, *408*, 181.

(4) Kuznetsov, M. L.; Pombeiro, A. J. L.; Dement'ev, A. I. *J. Chem. Soc., Dalton Trans.* **2000**, 4413.

(5) (a) Kostic, N. M.; Fenske, R. F. *J. Am. Chem. Soc.* **1981**, *103*, 4677. (b) Kostic, N. M.; Fenske, R. F. *Organometallics* **1982**, *1*, 489. (c) Kostic, N. M.; Fenske, R. F. *J. Am. Chem. Soc.* **1982**, *104*, 3879.

(6) Hofmann, P. In ref 1a, p 59.

(7) Ushio, J.; Nakatsuji, H.; Yonezawa, T. *J. Am. Chem. Soc.* **1984**, *106*, 5892.

(8) Poblet, J. M.; Strich, A.; West, R.; Bénard, M. *Chem. Phys. Lett.* **1986**, *126*, 169.

(9) Brower, D. C.; Templeton, J. L.; Mingos, D. M. P. *J. Am. Chem. Soc.* **1987**, *109*, 5203.

(10) Vyboishchikov, S. F.; Frenking, G. *Chem. Eur. J.* **1998**, *4*, 1439.

(11) Buil, M. L.; Eisenstein, O.; Esteruelas, M. A.; Garcia-Yebra, C.; Gutierrez-Puebla, E.; Olivan, M.; Oónate, E.; Ruiz, N.; Tajada, M. A. *Organometallics* **1999**, *18*, 4949.

(12) Guedes da Silva, M. F. C.; Lemos, M. A. N. D. A.; Fraústo da Silva, J. J. R.; Pombeiro, A. J. L.; Pellinghelli. M. A.; Tiripicchio, A. *J. Chem. Soc., Dalton Trans.* **2000**, 373.

(13) Almeida, S. S. P. R.; Pombeiro, A. J. L. *Organometallics* **1997**, *16*, 4469.

(14) Pombeiro, A. J. L. *New J. Chem.* **1997**, *21*, 649.

(15) Lemos, M. A. N. D. A.; Guedes da Silva, M. F. C.; Pombeiro, A. J. L. *Inorg. Chim. Acta* **1994**, *226*, 9.

(16) Pombeiro, A. J. L. In *Molecular Electrochemistry of Inorganic, Bioinorganic and Organometallic Compounds*; Pombeiro, A. J. L., McCleverty, J., Eds.; NATO ASI Series; Kluwer Academic Pulishers: Dordrecht, 1993; pp 331.

(17) Lemos, M. A. N. D. A.; Pombeiro, A. J. L. *J. Organomet. Chem.* **1988**, *356*, C79.

(18) Shustorovich, E. M.; Poraikoshits, M. A.; Buslaev, Yu. A. *Coord. Chem. Rev.* **1975**, *17*, 1.

Scheme 2. Synthesis of Isocyanide Complexes 2a−i via Acetonitrile Exchange Reactions

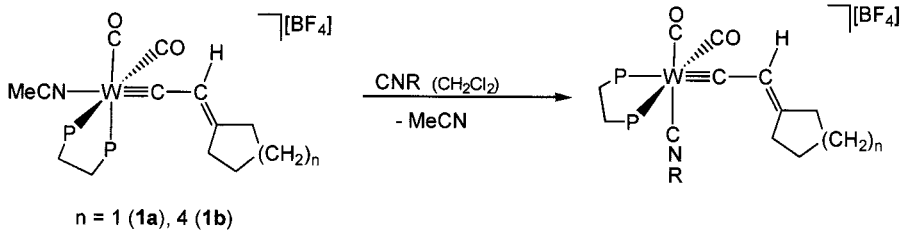

n = 1 (**1a**), 4 (**1b**)

R	n = 1,	4
Bu^n		**2a**
Bu^t	**2b**	**2c**
Cy	**2d**	**2e**
$PhCH_2$	**2f**	**2g**
$2,6\text{-}Me_2C_6H_3$	**2h**	**2i**

Table 1. Selected IR[a] and $^{31}P\{^1H\}$ and ^1H NMR Data for the Cationic Dicarbonyl Alkenyl-Carbyne Tungsten Complexes 2a−i

	IR		$^{31}P\{^1H\}$		^1H
complex	ν(CO)	ν(CN)	P *trans* to CO	P *cis* to CO	$C_\beta H$
2a	2008 (vs), 1948 (s)	2187 (m)	40.2 s (231.2)	21.3 s (83.8)	5.82 s,br
2b	2008 (vs), 1948 (s)	2172 (m)	39.4 s (230.5)	20.0 s (83.4)	5.97 s,br
2c	2007 (vs), 1948 (s)	2171 (m)	39.6 s (231.6)	20.3 s (83.4)	5.88 s,br
2d	2008 (vs), 1948 (s)	2176 (m)	39.9 s (229.8)	20.6 s (83.3)	5.92 s,br
2e	2007 (vs), 1948 (s)	2175 (m)	40.0 s (229.8)	20.8 s (83.4)	5.84 s,br
2f	2009 (vs), 1951 (s)	2181 (m)	40.1 s (232.2)	21.3 s (84.0)	5.90 s,br
2g	2009 (vs), 1951 (s)	2180 (m)	40.3 s (232.5)	21.6 s (83.9)	5.80 s,br
2h	2009 (vs), 1955 (s)	2137 (m)	40.2 s (236.2)	21.2 s (84.2)	5.98 s,br
2i	2009 (vs), 1955 (s)	2136 (m)	40.2 s (232.4)	21.4 s (85.1)	5.88 s,br

[a] Spectra recorded in CH_2Cl_2, ν (cm^{-1}). Abbreviations: m, medium; s, strong; vs, very strong. [b] Spectra recorded in $CDCl_3$, δ in ppm, J in Hz. Abbreviations: s, singlet; br, broad. [c] In parentheses, J(P−W).

Table 2. Selected $^{13}C\{^1H\}$ NMR Data for the Cationic Dicarbonyl Alkenyl-Carbyne Tungsten Complexes 2a−i[a]

complex	C_α[b]	C_β[c]	C_γ	CO *cis* to P[b]	CO *trans* to P[b]	W-*C*NR
2a	295.3 dd (24.6, 9.3)	136.4 d (16.7)	171.6 s	209.1 vr. t (7.2)	210.8 dd (25.1, 8.0)	146.5 m
2b	295.1 dd (24.3, 9.4)	d	172.3 s	208.7 dd (7.8, 6.6)	210.8 dd (25.2, 8.3)	143.5 m
2c	295.0 dd (24.5, 9.5)	136.4 d (16.7)	171.6 s	208.8 vr. t (7.2)	210.9 dd (25.4, 8.0)	144.0 m
2d	295.3 dd (24.8, 9.4)	*d*	172.2 s	208.8 vr. t (7.0)	210.7 dd (24.9, 7.7)	145.2 m
2e	295.2 dd (24.8, 9.5)	136.5 d (16.7)	171.7 s	209.0 vr. t (7.1)	210.9 dd (25.3, 8.4)	145.7 m
2f	295.9 dd (24.5, 9.2)	*d*	172.7 s	208.6 vr. t (7.4)	210.4 dd (25.2, 8.0)	148.1 m
2g	296.3 dd (23.9, 9.2)	137.1 d (16.9)	172.8 s	209.5 vr. t (6.6)	211.2 dd (25.3, 8.2)	149.4 m
2h	296.7 dd (23.6, 9.2)	*d*	173.5 s	207.5 vr. t (7.2)	210.3 dd (24.4, 8.2)	160.7 m
2i	297.3 dd (23.5, 9.1)	137.2 d (16.6)	173.4 s	208.3 vr. t (7.2)	211.2 dd (24.4, 8.2)	161.7 m

[a] Spectra recorded in $CDCl_3$, δ in ppm, J in Hz. Abbreviations: s, singlet; d, doublet; t, triplet; dd, doublet of doublet; m, multiplet; vr., virtual. [b] ^2J(C−P) (for the virtual triplets, ^2J(C−P) = ^2J(C−P')). [c] ^3J(C−P). [d] Overlapped by aromatic carbons.

broad signal for the alkenyl proton (=C_βH−) at δ 5.90−5.98 for the complexes with a five-membered ring (n = 1: **2b**, **2d**, **2f**, **2h**), while that in the complexes with the eight-membered ring (n = 4: **2a**, **2c**, **2e**, **2g**, **2i**) appears at a higher field (δ 5.80−5.88). ^{13}C NMR spectra display the expected alkenyl-carbyne carbon resonances (Table 2). In particular, the carbyne carbon resonance appears as a doublet of doublets at δ 295.0−297.3 [^2J(P−C) = 23.5−24.8, 9.1−9.5 Hz], confirming the proposed *trans* position of the carbyne groups with respect to one of the phosphorus atoms of the dppe ligand. Furthermore the ^{13}C NMR spectra also show the chemical inequivalence of the carbonyl groups *trans* and *cis* to the phosphorus atoms at δ 210.3−211.2 [^2J(P−C) = 24.4−25.4 Hz; 7.7−8.3 Hz] and δ 207.5−209.5 [^2J(P−C)= 6.6−7.2 Hz], respectively, along with the resonance of the W−C isocyanide group, which appears as a weak multiplet at δ 143.5−161.7.

The formation of complexes **2a**−**i** proceeds through an isomerization process. An analogous transformation has been observed in the synthesis of complexes **A** from the reaction of the tricarbonyl complexes **B** with the ligands L, proceeding via a monodentate diphosphine intermediate detected by NMR spectroscopy.[2h] However, this type of evidence was not obtained in the present study (e.g., by monitoring the reaction of **1a** with Bu^t-NC in $CDCl_3$ by $^{31}P\{^1H\}$ NMR, no intermediate was detected), and although the ligand exchange conceivably proceeds through the initial dissociation of the acetonitrile ligand *trans* to the carbyne group, the subsequent transformations are unknown. They can either occur similarly to the above case or follow other mechanistic possibilities, e.g. via isomerization of the five-coordinated intermediate formed upon acetonitrile loss, without rupture of a W−P bond. Nevertheless, the *trans* arrangement of two π-acceptor ligands with a high *trans*

Table 3. Cyclic Voltammetric Data[a] for the Cationic Alkenyl-Carbyne Complexes

[(dppe)(CO)$_2$(L)W{≡CCH=CCH$_2$CH$_2$(CH$_2$)$_n$CH$_2$}][BF$_4$] (L = MeCN, RNC, CO, PMe$_3$; n = 1 or 4) and [(dppe)(L)W{≡CCH=CCH$_2$CH$_2$(CH$_2$)$_n$CH$_2$}][BF$_4$] (L = κ^3-S$_2$CPCy$_3$)

complex	L	n	$^{I}E_{p/2}^{ox}$	$^{II}E_{p}^{ox}$	$^{I}E_{p}^{red}$	ref
1a[b]	MeCN	1	1.26	1.58	−1.58	2j
1b[b]	MeCN	4	1.22	1.59	−1.65	2j
2a	Bu^{n}NC	4	1.40		−1.44	this work
2b	Bu^{t}NC	1	1.35		−1.49	this work
2d	CyNC	1	1.38		−1.43	this work
2e	CyNC	4	1.41		−1.47	this work
2f	PhCH$_2$NC	1	1.44		−1.42	this work
2g	PhCH$_2$NC	4	1.45		−1.45	this work
2h	2,6-Me$_2$C$_6$H$_3$NC	1	1.41	1.72[c]	−1.38	this work
2i	2,6-Me$_2$C$_6$H$_3$NC	4	1.44	1.73[c]	−1.39	this work
3a[b]	CO	1	1.78		−1.08	2k
3b[b]	CO	4	1.71		−1.08	this work
4a	PMe$_3$	1	1.45	1.52[c]	−1.59	this work
5a[b]	κ^3-S$_2$CPCy$_3$	1	1.07	1.67	−1.66[d,e]	this work
5b[b]	κ^3-S$_2$CPCy$_3$	4	1.08	1.63	−1.63[d,f]	this work

[a] Potentials in V ± 0.02 vs SCE measured in 0.2 mol dm^{-3} [NBu$_4$][BF$_4$]/NCMe (CH$_2$Cl$_2$ for compounds **5a** and **5b**) at a scan rate of 0.2 V s^{-1} and at a Pt disk (d = 0.5 mm) electrode. Upon scan reversal following the cathodic wave, irreversible anodic waves are detected at potential values from −0.72 to −0.12 V. Addition of pyridine promotes the evolution of H$^+$ in the anodic processes, whose reduction is detected (at potential values ranging from ca. −0.3 to −0.6 V) on scan reversal following the anodic scan. [b] Included for comparative purposes. [c] Broad anodic wave with a lower peak current than the first anodic wave (I). [d] In THF, a second irreversible cathodic wave is detected at −1.91 V (process centered at the ligand). [e] At a scan rate of 1 V s^{-1} the wave becomes reversible, $E_{1/2}^{red}$ = −1.61 V. [f] At a scan rate of 1 V s^{-1} the wave becomes reversible, $E_{1/2}^{red}$ = −1.56 V.

influence is thermodynamically less stable than the *cis*, which is formed through a transient 16-electron species.

Electrochemical Studies

The electrochemical behaviors of the novel cationic alkenyl-carbyne isocyanide complexes **2a**−**i**, as well as of the related complexes **A** (L = PMe$_3$) (**4a**)[2h] and [(dppe)(κ^3-S$_2$CPCy$_3$)W{≡CCH=CCH$_2$CH$_2$(CH$_2$)$_n$CH$_2$}][BF$_4$] (**5a**, **5b**),[2i] have been studied by cyclic voltammetry (CV) and controlled potential electrolysis (CPE) at a platinum (or carbon)-disk or -gauze electrode, respectively. Relevant cyclic voltammetric data are given in Table 3, which, for comparative purposes, also includes the data of the precursor complexes (**1a**, **1b**)[2j,k,h] and the carbonyl complexes *mer*-[(dppe)(CO)$_3$W{≡CCH=CCH$_2$CH$_2$(CH$_2$)$_n$CH$_2$}][BF$_4$][2h,k] (**3a** and **3b**, the latter studied electrochemically in this work).

All the complexes undergo by CV one irreversible oxidation wave (I) ($^{I}E_{p/2}^{ox}$ in the range 1.07−1.78 V vs SCE), which, in some cases, is followed, at a higher potential, by a second one (II), broader and with a lower peak current. Wave I involves a single-electron transfer at sufficiently high scan rates, but on lowering the scan rate, it tends to a two-electron process as determined by CPE (see below). An irreversible single-electron cathodic wave is also detected at E_p^{red} in the range −1.38 to −1.66 V. For complexes **5** this cathodic wave presents a reversible character at scan rates higher than 1 V s^{-1}, but, by CPE, the cathodic process involves two

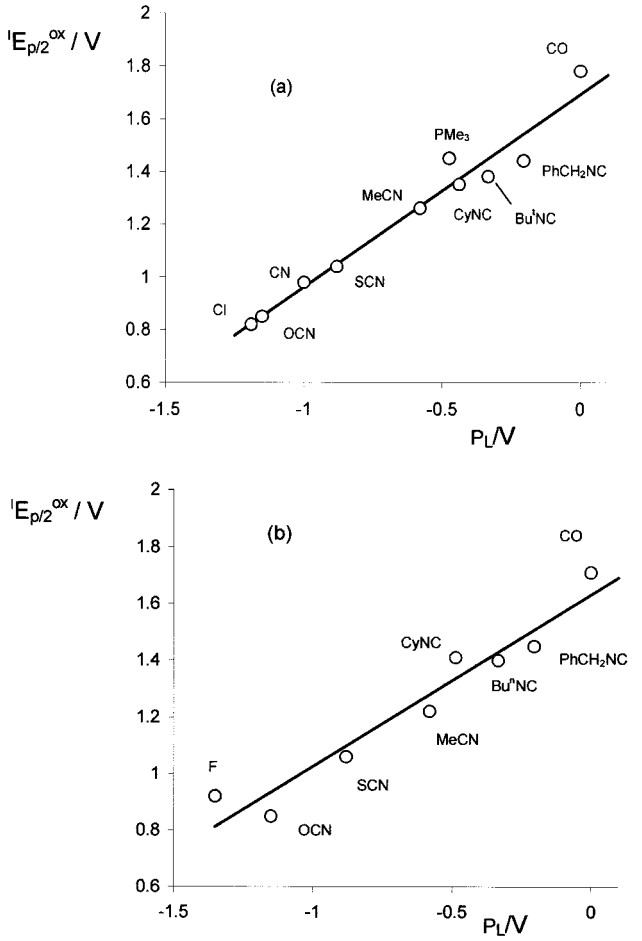

Figure 1. Plot of $^{I}E_{p/2}^{ox}$/V vs SCE for complexes [(dppe)(CO)$_2$(L)W(≡CCH=CCH$_2$CH$_2$(CH$_2$)$_n$CH$_2$)][BF$_4$] (L = MeCN,[2j,k] RNC, CO, or PMe$_3$) and [(dppe)(CO)$_2$(X)W(≡CCH=CCH$_2$CH$_2$(CH$_2$)$_n$CH$_2$)] (X = Cl, OCN, SCN, or CN)[2k] vs the electrochemical P_L ligand (L or X) parameter: (a) n = 1, $^{I}E_{p/2}^{ox}$ = 0.73P_L + 1.69 (correlation coefficient r = 0.979); (b) n = 4, $^{I}E_{p/2}^{ox}$ = 0.61P_L + 1.63 (correlation coefficient r = 0.967).

electrons; a second irreversible cathodic wave is observed for these complexes at ca. −1.9 V (in THF), and it conceivably involves a process centered at the phosphinodithiocarboxylate ligand.

The values of the oxidation potential of wave I for the isocyanide complexes **2** (1.35−1.45 V range) lie between those of the corresponding carbonyl (1.78 V **3a**[2k] or 1.71 V **3b**) and acetonitrile (1.26 V **1a** or 1.22 V **1b**)[2j] complexes, thus following the order (CO > CNR > NCR) of the net π-electron acceptor minus σ-donor character of these ligands, which is measured by the electrochemical P_L ligand parameter[19] (the stronger that character, the higher the P_L). This trend is clearly shown by the linear plot of $^{I}E_{p/2}^{ox}$ versus P_L for the series of the above cationic complexes **1**−**4** and the related neutral ones [(dppe)(CO)$_2$(X)W{≡CCH=CCH$_2$CH$_2$(CH$_2$)$_n$CH$_2$}] (X = Cl, OCN, SCN, or CN)[2k] with a common alkenyl-carbyne [n = 1 (Figure 1a) or 4 (Figure 1b)], in which P_L refers to the variable ligand (L or X) along the series. The P_L

(19) Chatt, J.; Kan, C. T.; Leigh, G. J.; Pickett, C. J.; Stanley, D. R. *J. Chem. Soc., Dalton Trans.* **1980**, 2032.

values for X[19] and L = MeCN,[19] CO,[19] or $CNBu^t$ [20] were taken from the literature, whereas those for L = $CNBu^n$, CNCy, $CNCH_2Ph$, or PMe_3 were estimated from the corresponding values of the E_L Lever ligand parameter[21] by using the relationship $P_L = 1.17E_L - 0.86$.[21]

An increase of the net π-acceptor minus σ-donor ability of the ligand (L or X) results in a stabilization effect on the HOMO of the complex, as confirmed by the theoretical studies discussed below and therefore in an anodic shift of the oxidation potential. Hence, the complexes with the neutral L ligands are oxidized at more anodic potentials than those with the anionic and stronger net electron donor X ligands, following the P_L order $Cl^- < OCN^- < CN^- < SCN^- <$ MeCN < CyNC < Bu^tNC < Bu^nNC < $PhCH_2NC$ < CO. The alkenyl-carbyne ligands are expected to have the highest P_L values, even higher than that of carbonyl ($P_L = 0$), since they behave as stronger π-electron acceptors than the latter ligand, as indicated by the more anodic oxidation potentials of the alkenyl-carbyne complexes of the study than that ($E_{1/2}^{ox} = 1.02$ V)[2j] of [W(CO)$_4$(dppe)]. The extensive π-electron acceptor character of other types of carbyne ligands (≡CCH_2R and ≡CNHR) has already been recognized electrochemically.[13,14,17]

The above linear plots correspond to the expression (eq 1) proposed by Pickett,[19] which relates the oxidation potential of the members of a series of 18-electron octahedral complexes [M_SL] (with a common {M_S} site) with P_L for the variable L ligand. E_S is a measure of the electron-richness of the metal site, given by the oxidation potential of the carbonyl complex [M_S(CO)] (the higher the E_S, the lower the electron-richness), and β is a measure of the polarizability of the metal site.

$$E^{ox}[M_SL] = E_S + \beta P_L(L) \qquad (1)$$

Therefore, from the intercept and the slope of the plots of Figure 1a,b, one can estimate the E_S and β parameters for the metal centers {M_S} of this study, {(dppe)-(CO)$_2$W(≡CCH=$\overline{CCH_2CH_2(CH_2)_nCH_2}$)}$^+$: $E_s = 1.69$ ($n = 1$) or 1.63 ($n = 4$) V, $\beta = 0.73$ ($n = 1$) or 0.61 ($n = 4$). These parameters have been recently estimated[2k] for the former center ($n = 1$) but by using a smaller number of points; therefore the values now proposed, obtained by considering also the additional data of the current work, are more reliable.

These metal centers are the first carbyne sites whose E_S and β parameters are reported. Compared with most of the other metal centers with known values[14,19,22] of these parameters [e.g., {W(CO)$_5$} exhibits $E_S = 1.50$ V (a high value) and $\beta = 0.90$],[22c] their electron-richness and polarizability are rather low (high E_S and low β values) and these features can be accounted for by considering the very strong π-electron acceptance ability of the alkenyl-carbyne and (although to a lesser extent) carbonyl ligands, with a resulting stabilization of the HOMO of the complex (high E_S) and its delocalization toward the carbyne (or CO) ligand as shown by MO calculations (see below and Figures 2 and 3), with an attenuating effect on changes of the HOMO energy (low β) upon variation of the L (or X) ligand.

From the plots of Figure 1 and the measured values (Table 3) of the oxidation potential for the 2,6-$Me_2C_6H_3$-NC complexes **2h** and **2i**, it is possible to estimate the P_L value of −0.36 V for this isocyanide ligand.

It is also noteworthy to mention that the complexes with the κ^3-S_2CPCy_3 (four-electron donor) ligand are oxidized [$E_{p/2}^{ox} = 1.07$ (**5a**) or 1.08 (**5b**) V] at a significantly lower anodic potential than those of the other cationic complexes, reflecting the stronger net electron-releasing character of the phosphinodithiocarboxylate ligand compared with CO and the other L (RCN, RNC, or PMe_3) ligands, although this evidence has to be taken cautiously since **5a** and **5b** are 16-electron complexes whereas the others follow the 18-electron count.

Controlled potential electrolysis at the anodic wave I of the isocyanide complexes normally involves about two electrons and leads to proton extrusion (overall $-2e^-/-H^+$ process) as a result of the oxidative promotion of the acidity of the alkenyl-carbyne ligand as observed in the anodically induced deprotonation of the related nitrile (**1**), halide, or pseudo-halide complexes[2j,k] and of the aminocarbyne *trans*-[ReCl(CNH$_2$)(dppe)$_2$]$^+$.[12,15] The liberated proton is detected by its broad CV cathodic wave at E_p^{red} ca. −0.3 to −0.6 V (which undergoes an extensive cathodic shift on replacement of Pt by vitreous carbon as the working electrode material) and by potentiometric titration of the electrolyzed solutions.

On the time scale of CV, for sufficiently low scan rates, the anodically induced H^+ loss also occurs as shown by the detection of the protic cathodic wave on reverse of the anodic scan following the oxidation wave. The anodic current-function $i_p^{ox}C^{-1}v^{-1/2}$ (i_p^{ox} = anodic peak current, C = concentration, v = scan rate), which at sufficiently high scan rates corresponds to a single-electron transfer, increases, as observed[2j,k] for other alkenyl-carbyne complexes, on lowering the scan rate and on addition of pyridine, being consistent with an electrode process comprising, at lower scan rates, more than one electron with coupled proton loss.

Theoretical Studies

The theoretical studies performed on the model complexes *trans*- and *cis*-[(PH$_3$)$_2$(CO)$_2$(L)W(≡CCH=CH_2)]$^{m+}$ [L = Cl^- ($m = 0$) ***trans*-1** or ***cis*-1**; L = NCMe ($m = 1$) ***trans*-2** or ***cis*-2**; L = CNMe ($m = 1$) ***trans*-3** or ***cis*-3**; L = CO ($m = 1$) ***trans*-4** or ***cis*-4**] (Scheme 3) were aimed to get a rationale for (i) the dependence of the relative stability of the stereoisomers on the ligand *trans* to the carbyne group, (ii) the mechanism of the *trans*-to-*cis* isomeric conversion that occurred in the ligand exchange of NCMe by CNR, (iii) the understanding of the chemical bond properties, and (iv) the order of the values of the oxidation potential of the complexes.

Selected results of geometry optimization are presented (Table 4), as well as molecular orbital diagrams

(20) Pombeiro, A. J. L.; Pickett, C. J.; Richards, R. L. *J. Organomet. Chem.* **1982**, *224*, 285.
(21) Lever, A. B. P. *Inorg. Chem.* **1990**, *29*, 1271.
(22) (a) Guedes da Silva, M. F. C.; Fraústo da Silva, J. J. R.; Pombeiro, A. J. L.; Pellinghelli, M. A.; Tiripicchio, A. *J. Chem. Soc., Dalton Trans.* **1996**, 2763. (b) Wang, Y.; Pombeiro, A. J. L. *Port. Electrochim. Acta* **1993**, *11*, 111. (c) Facchin, G.; Mozzon, M.; Michelin, R. A.; Ribeiro, M. T. A.; Pombeiro, A. J. L. *J. Chem. Soc., Dalton Trans.* **1992**, 2827. (d) Carvalho, M. F. N. N.; Pombeiro, A. J. L. *J. Chem. Soc., Dalton Trans.* **1989**, 1209. (e) Carriedo, G. A.; Riera, V.; Connelly, N. G.; Raven, S. J. *J. Chem. Soc., Dalton Trans.* **1987**, 1769. (f) Pombeiro, A. J. L. *Inorg. Chim. Acta* **1985**, *103*, 95. (g) Pombeiro, A. J. L.; Pickett, C. J.; Richards, R. L. *J. Organomet. Chem.* **1982**, *224*, 285.

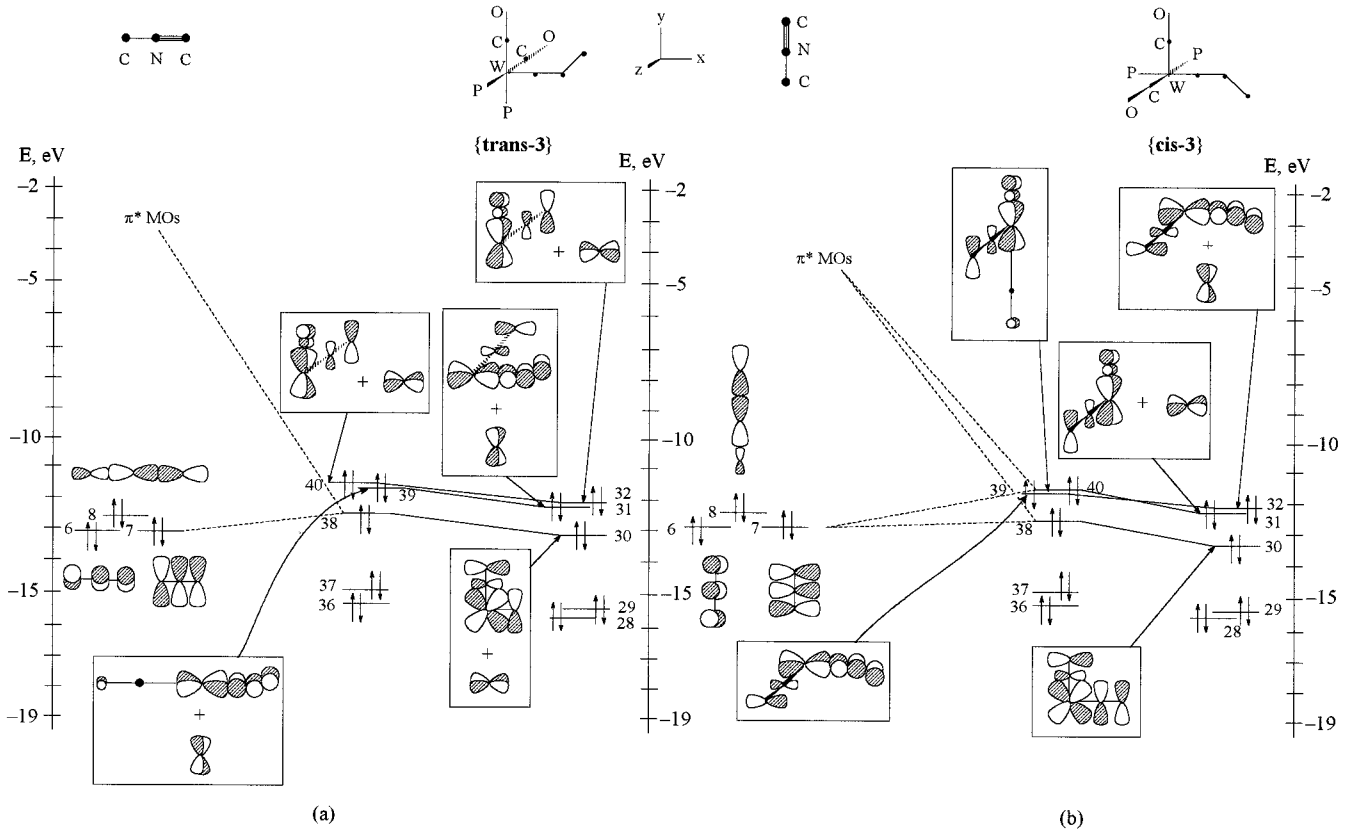

Figure 2. MO diagram for the (a) ***trans*-3** and (b) ***cis*-3** complexes.

for the isocyanide complexes (Figure 2), the composition of the HOMOs (Figure 3), the energies of the valence orbitals (Table 5), and the total energies (Table 6).

(a) Equilibrium Structural Parameters. The structural parameters calculated for the *trans*-chlorocomplex ***trans*-1** are in agreement with those reported[2h] in the X-ray diffraction analysis for *trans*-[(dppe)$(CO)_2$(Cl)W-{≡CCH=CCH$_2$CH$_2$CH$_2$CH$_2$}], and selected bond lengths are shown in Table 4 together with those obtained for the other model complexes.

The W−L (L = Cl^-, NCMe, CNMe, or CO) bond length is always longer in the *trans* isomers than in the corresponding *cis* ones (by ca. 0.04, 0.11, 0.18, or 0.28 Å, respectively), reflecting a strong *trans* influence of the alkenyl-carbyne ligand, which, for the *cis* isomers, also accounts for the longer (by ca. 0.18−0.25 Å) W−P distance for the PH_3 ligand *trans* to the carbyne (W−P2) in comparison with that for the *cis*-PH_3 (W−P3). Within the alkenyl-carbyne framework, W≡C(14)−C(15)H=C(17)H_2, the W≡C(14), C(14)−C(15), and C(15)=C(17) bond lengths correspond to the expected triple, single, and double bond characters (average values of 1.82, 1.43, and 1.33 Å, respectively) and are not significantly affected by changing the ligand in the *trans* position.

The isocyanide ligand in both complexes ***trans*-3** and ***cis*-3** is linear and presents a C≡N bond length, 1.146 Å (average for both isomers), shorter than that, 1.158 Å, for free CNMe calculated by the same approach (estimated bond orders of 2.58 and 2.35, respectively). These features agree with the experimentally observed shift to higher wavenumbers (as often found[23] for isocyanide complexes) of ν(C≡N) of the isocyanides upon coordination in complexes **2a**−**i** (Table 1) and indicate that the σ-electron donor component (*a*) of the W−CNR bond predominates over the π-electron acceptor one (*b*). This behavior is also in accord with the relatively long calculated W−CNMe bond lengths (Table 4) and can be accounted for by the effective competition of the alkenyl-carbyne and carbonyl co-ligands (with a strong π-acceptor ability) for the available metal d_π electrons.

(a) *(b)*

Nevertheless, a hardly detected π-electron acceptance of the CNMe ligand in ***trans*-3** and ***cis*-3** is suggested by the minor elongation of the coordination bond of the π-acceptor ligand (CO or alkenyl-carbyne) in *trans* position; that is, the W−C(10)O distance in ***cis*-3** (CO *trans* to CNMe) is longer by ca. 0.03 Å than in ***trans*-3** (CO *trans* to PH_3), and the W≡C(14) bond length in ***trans*-3** (carbyne *trans* to CNMe) is longer by ca. 0.01−0.02 Å than in ***cis*-3**, in ***trans*-2**, or in ***trans*-1** (carbyne *trans* to PH_3, NCMe, or Cl^-, respectively).

Carbon monoxide is the ligand that is structurally more affected by the alkenyl-carbyne, in consistency with its strongest π-electron accepting character compared to the other L ligands. Hence, for the CO ligand *trans* to the carbyne (***trans*-4**), the W−C(20)O(21) and

(23) Nakamoto, K. *Infrared and Raman Spectra of Inorganic and Coordination Compounds*, 5th ed.; Wiley-Interscience: New York, Part B, 1997.

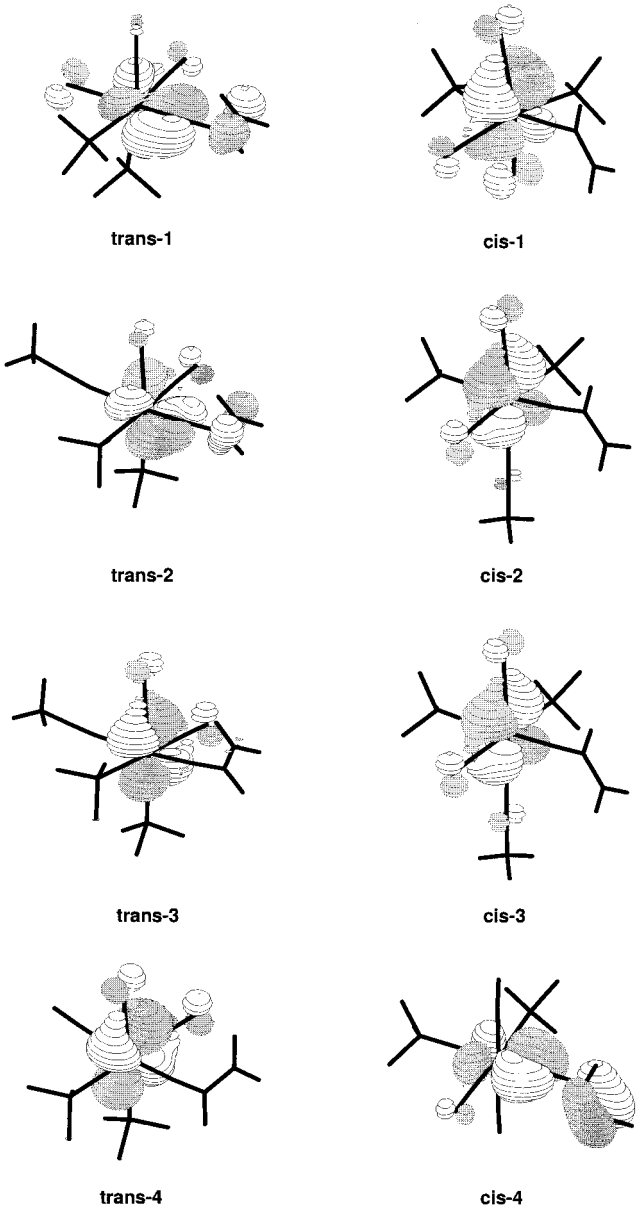

Figure 3. MOLDEN plots for the HOMOs of the model complexes.

the C(20)−O(21) distances are longer (by 0.28 Å) and shorter (by 0.01 Å), respectively, than the corresponding distances for the ***cis*-4** isomer. The π-acceptance of CO is also reflected in the slightly longer W−CO distance (by ca. 0.05 Å) of the two mutually *trans* CO ligands, C(10)O(12) and C(20)O(21), in ***cis*-4**, in comparison with the C(11)O(13) ligand which is *trans* to PH_3.

The lengths of the W−C(14) (for the *trans* complexes) or W−C(10) (for the *cis* ones) bonds that are *trans* to L increase from L = Cl^- to CO in accord with the order of π-electron acceptance of the latter ligand. As expected, the C(10)−O(12) bond length follows the opposite trend.

(b) Molecular Orbital Analysis. The molecular orbital (MO) diagrams have been established for all the optimized structures by considering them derived from coupling of L (Cl^-, NCMe, CNMe, or CO) with the coordinatively unsaturated metal fragment $\{(PH_3)_2(CO)_2W(\equiv CCH{=}CH_2)\}^+$ with the same geometrical parameters as the corresponding complex molecule. This fragment is denoted by {***trans***} or {***cis***} when corresponding to the *trans* or the *cis* isomer of the complex, respectively. Figure 2 shows the diagrams for the isocyanide isomers ***trans*-3** and ***cis*-3**.

All {***trans***} fragments have very similar valence MO composition, with the HOMO (32 MO, Figure 2) resulting mainly from the linear combination of d_{yz} (W) with π^* and π orbitals of the CO ligands (the π^* contribution predominating over that of π) and presenting W−CO bonding and C−O antibonding characters, thus reflecting the π-electron acceptance of the CO ligands. The various {***cis***} fragments also exhibit analogous MO diagrams, with the HOMO (32 MO, Figure 2) resulting mainly from the combination of d_{xz} (W) with the p_z orbitals of the carbyne ligand C(14)C(15)H=C(17)H_2 [bonding W−C(14) and C(15)−C(17) combinations and antibonding for C(14)−C(15)] and with $\pi \pm \pi^*$ of the coplanar CO ligand (predominance of the π^* contribution).

The next occupied MO of {***trans***} (31 MO) reflects mainly the bonding combination of tungsten d orbitals with p orbitals of the carbyne ligand carbons and the interaction of d orbitals with π^* and π of one or two (for {***trans*-4**}) CO ligands (with predominance of the π^* contribution over that of π). The interaction of W, CO, and $CCHCH_2$ (for {***cis*-1**} and {***cis*-2**}) orbitals is observed also for the 31 MO of {***cis***}. Hence, the carbonyls can form a noticeable π-interaction with the d_π (metal) orbitals that are in the plane of the carbyne ligand (d_{xz} or d_{xy}) (the contribution of CO orbitals in such interaction can reach 5.4%), thus competing with the latter ligand for the π-electron release from the metal.

The next MO (30 MO) reflects mainly the interaction of $d_{xy} \pm d_{xz}$ (W) (for {***trans***}) or d_{xy} (W) (for {***cis***}) with the linear combination $\pi \pm \pi^*$ of CO ligands and the bonding interaction of metal-d orbitals with $p_y + p_z$ of the carbyne carbon atom. Thus, the 30 and 31 MOs ({***trans***}) or the 30 and 32 MOs ({***cis***}) of the metal fragment account for the two π-components of the coordination bond of the carbyne ligand.

Within the alkenyl-carbyne ligand C(14)C(15)H=C(17)H_2, the respective HOMO has a C(14)−C(15) antibonding character and is bonding between the olefinic carbons C(15)=C(17), consistent with the single and double bond characters of these bonds.

The valence-occupied MOs of *trans*- and *cis*-$[(PH_3)_2(CO)_2(L)W(\equiv CCH{=}CH_2)]^{m+}$ (L = Cl^-, $m = 0$; L = NCMe, CNMe, CO; $m = 1$) mainly correspond to those of the respective metal fragments, the L ligands providing only small contributions, which, however, are significantly higher for the *cis* than for the *trans* isomers.

The total contributions of L = CNMe and NCMe in the corresponding complexes are very small for the two highest occupied MOs (40 and 39, Figure 2 for the former complexes; see also Figure 3 for the HOMOs), reflecting the weak π-acceptance properties of these ligands compared with the carbyne. That is also indicated by Figure 3 with the graphical representations of the HOMOs for all the models. Despite the strongest π-acceptance of CO in comparison with the other L ligands, the contribution of L (CO) orbitals is virtually null in the HOMO (Figure 3) either for ***trans*-4** or for ***cis*-4**, due to the orthogonal orientation of the respective d(W) and p(L = CO) orbitals. Moreover, the total contribution of CO orbitals for the next occupied MO of ***trans*-4** is also small (1.2%) despite the coplanarity of

Scheme 3. Model Compounds and Atomic Labeling Scheme[a]

A

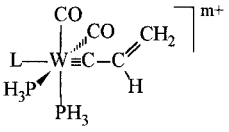

L	m	
Cl^-(20)	0	**trans-1**
N(20)C(21)C(22)H_3	1	**trans-2**
C(20)N(21)C(22)H_3	1	**trans-3**
C(20)O(21)	1	**trans-4**

B

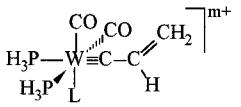

L	m	
Cl^-(20)	0	**cis-1**
N(20)C(21)C(22)H_3	1	**cis-2**
C(20)N(21)C(22)H_3	1	**cis-3**
C(20)O(21)	1	**cis-4**

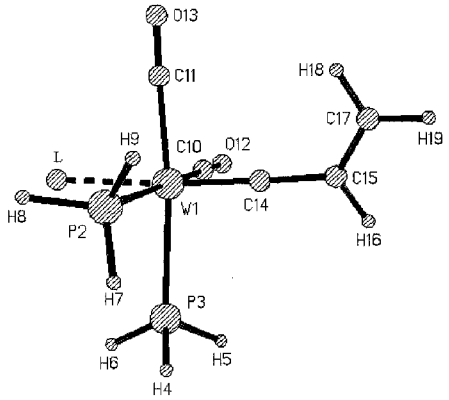

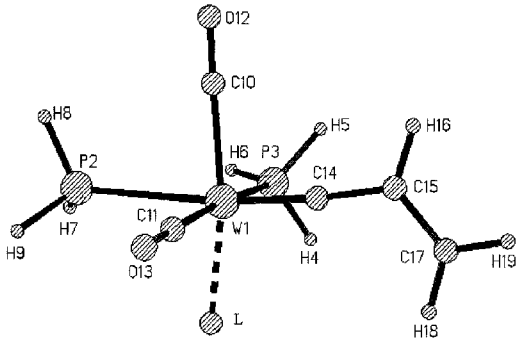

[a]The corresponding metal centers, without the L ligand, are denoted similarly, but within braces, i.e., {***trans*-1**}, {***cis*-1**}, etc.

Table 4. Selected Bond Lengths (Å) for Calculated Structures

	***trans*-1**	***cis*-1**	***trans*-2**	***trans*-2′**	***cis*-2**	***cis*-2′**	***trans*-3**	***trans*-3′**	***cis*-3**	***cis*-3′**	***trans*-4**	***trans*-4′**	***cis*-4**	***cis*-4′**
W−C14	1.813	1.808	1.818	1.817	1.816	1.818	1.829	1.827	1.819	1.822	1.829	1.829	1.826	1.833
W−C11	2.067	2.065	2.070	2.072	2.064	2.071	2.069	2.071	2.067	2.074	2.071	2.073	2.084	2.095
W−C10	2.066	2.025	2.067	2.069	2.056	2.049	2.065	2.068	2.091	2.084	2.070	2.069	2.129	2.114
W−L	2.641	2.605	2.364	2.368	2.251	2.256	2.400	2.399	2.221	2.220	2.413	2.398	2.130	2.116
W−P2	2.666	2.906	2.667	2.642	2.884	2.838	2.665	2.640	2.862	2.821	2.673	2.645	2.848	2.802
W−P3	2.668	2.652	2.671	2.649	2.666	2.640	2.671	2.645	2.666	2.643	2.673	2.651	2.669	2.648
C14−C15	1.440	1.437	1.435	1.436	1.435	1.435	1.433	1.434	1.434	1.434	1.429	1.430	1.430	1.428
C15−C17	1.331	1.332	1.332	1.332	1.332	1.332	1.333	1.333	1.332	1.332	1.334	1.334	1.333	1.335
C10−O12	1.137	1.147	1.135	1.135	1.137	1.139	1.135	1.135	1.133	1.134	1.133	1.134	1.128	1.130
C11−O13	1.137	1.136	1.135	1.135	1.135	1.134	1.135	1.135	1.135	1.135	1.133	1.134	1.131	1.130
N20−C21			1.139	1.139	1.138	1.138								
C21−C22			1.458	1.458	1.458	1.458								
C20−N21							1.145	1.145	1.147	1.148				
N21−C22							1.439	1.439	1.437	1.437				
C20−O21											1.117	1.118	1.128	1.130

Table 5. Energies (eV) of Valence Molecular Orbitals for the Model Complexes *trans*- or *cis*-$[(PH_3)_2(CO)_2(L)W(\equiv CCH{=}CH_2)]^{m+}$ (*trans* or *cis*), Energies of the HOMO for the Corresponding Metal Fragments $\{(PH_3)_2(CO)_2W(\equiv CCH{=}CH_2)\}^+$ {*trans*} or {*cis*}, and Difference of the HOMO Energies $\Delta E = E_{HOMO}$(complex) − E_{HOMO}(metal fragment)

	Cl^- ($m = 0$)		CH_3CN ($m = 1$)		$CNCH_3$ ($m = 1$)		CO ($m = 1$)	
	***trans*-1**	***cis*-1**	***trans*-2**	***cis*-2**	***trans*-3**	***cis*-3**	***trans*-4**	***cis*-4**
LUMO	0.69	0.72	−1.87	−1.87	−2.03	−1.91	−2.86	−2.50
HOMO	−8.21	−7.98	−11.29	−11.21	−11.39	−11.36	−11.96	−12.09
	{***trans*-1**}	{***cis*-1**}	{***trans*-2**}	{***cis*-2**}	{***trans*-3**}	{***cis*-3**}	{***trans*-4**}	{***cis*-4**}
HOMO	−12.10	−12.18	−12.10	−12.12	−12.11	−12.08	−12.09	−11.98
ΔE	3.89	4.20	0.81	0.91	0.72	0.72	0.13	−0.11

the appropriate d(W) and p(CO) orbitals, a behavior that is consistent with the strong *trans*-influence of the carbyne ligand (see above); in accord, for ***cis*-4**, such a contribution is quite significant (6.2%), being identical to that of the C(10)O(12) ligand. The total contribution of nonhydrogen MOs of L to three highest occupied MOs increases from ***cis*-2** to ***cis*-4** (4.6% NCMe, 6.8% CNMe, 10.3% CO).

The chloride ligand (p orbitals) provides the greatest contribution (in comparison with the other ligands L) to the HOMO (6.5% or 9.7% for ***trans*** or ***cis***, respectively), which, however, has a W−Cl antibonding char-

Table 6. Difference of the Total Energies ΔE of the *trans* and the *cis* Isomers (eV)

	$\Delta E = E_{trans} - E_{cis}$ (eV)	
isomeric pair	HF	MP2
***trans*-1/*cis*-1**	−0.27	−0.28
***trans*-2/*cis*-2**	−0.13	−0.15
***trans*-2′/*cis*-2′**	−0.19	
***trans*-3/*cis*-3**	0.12	0.11
***trans*-3′/*cis*-3′**	0.05	
***trans*-4/*cis*-4**	0.37	0.37
***trans*-4′/*cis*-4′**	0.38	

acter (Figure 3). The next occupied MO does not include a significant contribution of the Cl^- ligand due to the orthogonal orientation of the appropriate d(W) and p(Cl) orbitals.

The calculated energy of the HOMO (Table 5) for the complexes follows the order **1** (L = Cl^-) > **2** (L = NCMe) > **3** (L = CNMe) > **4** (L = CO). The destabilization of the HOMO of the metal fragment (except for ***cis*-4**) as a result of its interaction with the appropriate L orbitals to form the complex, $\Delta E = E_{HOMO}$(complex) − E_{HOMO}(metal fragment) (Table 5 and Scheme 4), increases in the opposite order, i.e., from L = CO to L = Cl^-. The variation of the HOMO energy of the complex, as a result of changing L, is greater for the *cis* than for the *trans* isomers, in accord with the greater participation of the L ligand orbitals in the HOMOs of the former isomers (see above), leading to a reverse of their energy levels, in agreement with the relative stabilities of these isomers (see below).

The order of the calculated energies of the HOMO of the model complexes corresponds to that of the net σ-electron donor minus π-acceptor ability of L (L = Cl^- > NCMe > CNMe > CO) and is consistent with the measured oxidation potential of the complexes (see above), which decreases with the destabilization of the HOMO, i.e., from L = CO to L = Cl^-. Moreover, an isomeric dependence of the oxidation potential can be predicted (see Scheme 4), a behavior that had not yet been reported for carbyne complexes, although being known,[24] for example, for octahedral-type carbonyl,[25] isocyanide,[26] and nitrile[27] complexes.

(c) Relative Isomeric Stabilities. It was experimentally observed that the *trans* isomer is the obtained one when L does not behave as an appreciable π-electron acceptor, such as Cl^- (without a π-accepting character) or NCMe, whereas the *cis* geometry is more stable for L = CNMe or CO, which are weaker net electron donors with a known usual π-electron withdrawing ability, thus avoiding their competition with the carbyne for the metal d_π electrons. That is fully supported by the values of the total energies of the various optimized structures at HF and MP2 approaches (Table 6), which show that ***trans*-1** (L = Cl^-) and ***trans*-2** (L = NCMe) are more stable than the corresponding *cis* structures, whereas the reverse occurs for the CNMe and CO complexes (***cis*-3** and ***cis*-4** are more stable than the corresponding *trans* isomers). The calculations predict that the acetonitrile complexes should be more stable than the isocyanide ones. This seems to indicate that the observed formation of the isocyanide derivatives through exchange reactions is kinetically controlled due to the high lability of the precursor acetonitrile complexes.

In addition, the energy difference between the two complex isomers ($E_{trans} - E_{cis}$) increases in the order L = Cl^- < NCMe < CNMe < CO. This parallels (for the species with unsaturated L) the increase of the contribution of π^* MOs (L) to the valence-occupied MOs of the complexes (i) in the same order and (ii) from the *trans* to the *cis* geometry, corresponding to an enhancement of the π-back-donation from the metal to the unsaturated L ligand. That trend also reflects the higher relative destabilization of the *trans* isomer by the strongest π-electron acceptor (CO) in *trans* position to the carbyne.

The contribution of L π MOs to the valence-occupied MOs of the complexes can also play a significant role, and for example for L = NCMe it increases from the *trans* to the *cis* isomer with a concomitant increase of the W−NCMe antibonding combination with resulting destabilization of the coordination bond of the ligating acetonitrile. For L = CO, the relative contribution of π^* MOs of CO increases from *trans* to *cis* isomers and the bonding W−L interaction rises from ***trans*-4** to ***cis*-4**.

To take into account the chelating effect from the bidentate dppe ligand in the real complexes, which can affect the relative stability of the geometrical isomers, the full geometry optimization of the model structures *trans*- and *cis*-$[(H_2PCH_2CH_2PH_2)(CO)_2(L)W(\equiv CCH{=}CH_2)]^+$ (***trans*-2′** and ***cis*-2′** for L = NCMe; ***trans*-3′** and ***cis*-3′** for L = CNMe; ***trans*-4′** and ***cis*-4′** for L = CO) with the bidentate ligand $H_2PCH_2CH_2PH_2$ was also performed. The composition and energies of the frontier molecular orbitals and the structural parameters of each isomer of **2′**, **3′**, and **4′** are similar to those for **2**, **3**, and **4**, respectively, except the bond angles at the metal atom and the W−P distances, which are shorter for the former complexes than for the latter by ca. 0.02−0.04 Å (Table 4). The comparison of the total energies of the geometrical isomers for the bidentate phosphine models shows that for the nitrile complex the *trans*-isomer (***trans*-2′**) is more stable than the *cis*-one (***cis*-2′**), whereas the reverse of the relative isomeric stability occurs for the isocyanide (**3′**) and carbonyl (**4′**) complexes (although the energy difference is lower in the case of **3′** than in that of **3**), in agreement with the above results obtained for the monodentate PH_3 complexes **2**, **3**, and **4** (Table 6). Thus, the similarity of the geometrical and electronic structures of the models with mono- and bidentate phosphine ligands and the good agreement with the experimentally observed relative isomeric stability corroborate the validity of the use, in these

(24) For reviews see: (a) Pombeiro, A. J. L.; Guedes da Silva, M. F. C.; Lemos, M. A. N. D. A. *Coord. Chem. Rev.*, submitted for publication. (b) Bond, A. M.; Colton, R. *Coord. Chem. Rev.* **1977**, *166*, 161.

(25) (a) Bond, A. M.; Colton, R.; Humphrey, D. G.; Mahon, P. J.; Snook, G. A.; Tedesco, V.; Walter, J. N. *Organometallics* **1998**, *17*, 2977. (b) Bond, A. M.; Colton, R.; Cooper, J. B.; Traeger, J. C.; Walter, J. N.; Way, D. M. *Organometallics* **1994**, *13*, 3434. (c) Cummings, D. A.; McMaster, J.; Rieger, A. L.; Rieger, P. H. *Organometallics* **1997**, *16*, 4362. (d) Abdel-Hamid, R.; El-Samahy, A. A.; Rabia, M. K. M.; Taylor, N.; Shaw, B. L. *Bull. Chem. Soc. Jpn.* **1994**, *67*, 321. (e) Guedes da Silva, M. F. C.; Ferreira, C. M. P.; Fraústo da Silva, J. J. R.; Pombeiro, A. J. L. *J. Chem. Soc., Dalton Trans.* **1998**, 4139.

(26) Guedes da Silva, M. F. C.; Hitchcock, P. B.; Hughes, D. L.; Marjani, K.; Pombeiro, A. J. L.; Richards, R. L. *J. Chem. Soc., Dalton Trans.* **1997**, 3725.

(27) (a) Guedes da Silva, M. F. C.; Fraústo da Silva, J. J. R.; Pombeiro, A. J. L.; Amatore, C.; Verpeaux, J.-N. *Organometallics* **1994**, *13*, 3943. (b) Guedes da Silva, M. F. C.; Fraústo da Silva, J. J. R.; Pombeiro, A. J. L.; Amatore, C.; Verpeaux, J.-N. *Inorg. Chem.* **1998**, *37*, 2344.

Scheme 4. Relative Energy of the HOMO, $\Delta E = E_{HOMO}$(complex) − E_{Homo}(fragment) (eV)

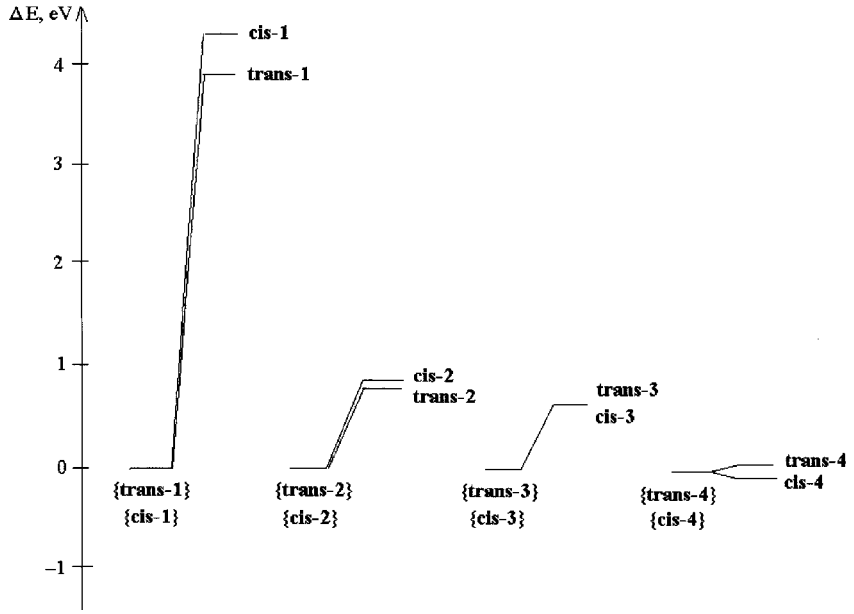

systems, of two monodentate PH_3 ligands as a model for the chelating dppe.

Concluding Remarks

Novel cationic isocyanide alkenyl-carbyne Fischer-type tungsten complexes with such ligands in mutually *cis* position were prepared from the corresponding *trans* acetonitrile alkenyl-carbyne precursors via an acetonitrile exchange reaction and subsequent *trans*-to-*cis* isomerization. They belong to a scarce type of unsaturated carbyne complexes, and the work provided an opportunity to investigate, by electrochemical and ab initio quantum-chemical methods, the electronic properties of the alkenyl-carbyne ligands and their effects, as well as of *trans*- and *cis*-L co-ligands (L = Cl^-, NCMe, CNMe, CO), on the properties of the complexes.

The alkenyl-carbyne ligands (i) are rather strong π-electron acceptors, (ii) contribute appreciably to the highest or the next occupied MO which displays bonding metal≡C, antibonding C−CH, and bonding CH=CH_2 characters along the W≡C−CH=CH_2 framework, (iii) confer a low electron-richness and a low polarizability to the metal centers they belong to (thus not only behaving as effective electron-withdrawing ligands but also presenting a high capacity to buffer changes in the electronic density of the metal upon change of a co-ligand L), and (iv) exhibit a considerable *trans* influence, which increases with the competing π-electron acceptor character of the *trans* ligand (L).

The *trans* isomer is more stable than the *cis* when L behaves either as a π-electron donor (Cl^-) or a weak π-electron acceptor (NCMe), whereas the reverse of the relative isomeric stability occurs when L is an effective π-electron acceptor (CNMe or CO), in accord with the experimentally obtained products.

The π-electron acceptance of the L ligand leads to a stabilizing effect of the HOMO of the complex, in agreement with the increase of the oxidation potential, and the effect is more pronounced for the *cis* than for the *trans* isomers in view of the greater participation of the L orbitals in the HOMOs of the former isomers. Hence, an isomeric dependence of the oxidation potential is predicted for the first time for carbyne complexes.

Experimental Section

The reactions were carried out under dry dinitrogen using Schlenk techniques. All solvents were dried by standard methods and distilled under dinitrogen before use. The precursor complexes *trans*-[(dppe)$(CO)_2$(MeCN)W{≡CCH=$\overline{CCH_2(CH_2)_nCH_2CH_2}$}][$BF_4$] ($n$ = 1 (**1a**), 4 (**1b**)) were prepared by the literature method.[2h] Isocyanides RNC (R = Bu^n, Bu^t, Cy, $PhCH_2$, 2,6-$Me_2C_6H_3$) (Aldrich Chemical Co.) were used as received.

Infrared spectra were recorded on a Perkin-Elmer 1720-XFT spectrometer. Mass spectra (FAB) were recorded using a VG-Autospec spectrometer, operating in the positive mode; 3-nitrobenzyl alcohol (NBA) was used as the matrix. The conductivity was measured at room temperature, in ca. 10^{-3} mol dm^{-3} acetone solution, with a Jenway PCM3 conductivimeter. The C, H, and N analyses were carried out with a Perkin-Elmer 240-B microanalyzer.

NMR spectra were run on a Bruker AC300. The instrument was configured with a triple probe (^1H, ^{13}C, ^{31}P). The inner coil was doubly tuned for ^1H and ^{31}P, and the outer coil was tunable in the frequency range 18−160 MHz. The spectral references used were tetramethylsilane (TMS) for ^1H and ^{13}C and 85% H_3PO_4 for ^{31}P (s = singlet, d = doublet, vr. t = virtual triplet, m = multiplet, br = broad, dd = doublet of doublets).

Selected IR and ^1H, $^{13}C\{^1H\}$, and $^{31}P\{^1H\}$ NMR spectroscopic data for the novel alkenyl-carbyne tungsten complexes are collected in Tables 1 and 2 and are not repeated in the following descriptions.

Synthesis of Cationic Alkenyl-Carbyne Tungsten Complexes *cis*-[(dppe)$(CO)_2$(RNC)W{≡C−CH=$\overline{CCH_2(CH_2)_nCH_2CH_2}$}][$BF_4$] [R = Bu^n, n = 1 (2a); R = Bu^t, n = 1 (2b), 4 (2c); R = Cy, n = 1 (2d), 4 (2e); R = $PhCH_2$, n = 1 (2f), 4 (2g); R = 2,6-$Me_2C_6H_3$, n = 1 (2h), 4 (2i)]. One equivalent of the corresponding isocyanide was added to a solution of **1a** or **1b** (0.2 mmol) in 10 mL of dichloromethane. The mixture was stirred at room temperature. The reaction was followed by infrared in the carbonyl region until the total disappearance of the starting material. After ca. 2 h only the *cis*-dicarbonyl and isocyanide absorptions of the desired com-

pound were observed. The resulting orange solution was evaporated to dryness. The orange-red tar was washed with diethyl ether (2 × 5 mL) and hexane (2 × 5 mL). Drying in vacuo gave an orange solid. Yield: **2a**, 92%; **2b**, 85%; **2c**, 85%; **2d**, 86%; **2e**, 88%; **2f**, 85%; **2g**, 85%; **2h**, 88%; **2i**, 90%. Conductivity (acetone, 20 °C, Ω^{-1} cm^2 mol^{-1}): **2a**, 125; **2b**, 122; **2c**, 117; **2d**, 118; **2e**, 129; **2f**, 120; **2g**, 127; **2h**, 128; **2i**, 124.

Spectral and analytical data for **2a**: ^{1}H NMR (δ, $CDCl_3$) 0.66 [t, J(H−H) = 6.4 Hz, 3H, CH_3], 0.75−1.00 (m, 4H, $CNCH_2CH_2$-CH_2−), 1.50 (m, 6H, 3 CH_2), 1.76 (m, 4H, 2 CH_2), 2.14 (m, 2H, CH_2), 2.59 (m, 2H, CH_2), 2.80−3.30 [m, 4H, $P(CH_2)_2P$], 3.06 [t, J(H−H) = 6.4 Hz, 2H, $CNCH_2$-], 7.44−7.82 (m, 20H, 2 PPh_2); $^{13}C\{^1H\}$ NMR (δ, $CDCl_3$) 12.9 (s, CH_3), 19.1 (s, CH_2), 25.4 (s, CH_2), 25.0−27.9 [m, $P(CH_2)_2P$], 26.3 (s, CH_2), 26.7 (s, CH_2), 27.1 (s, CH_2), 27.6 (s, CH_2), 29.9 (s, CH_2), 32.7 (s, CH_2), 38.9 (s, CH_2), 43.9 (s, $CNCH_2$-), 128.6−133.6 (m, 2 PPh_2). Anal. Calcd for $C_{43}H_{48}BF_4NO_2P_2W$: C, 54.7; H, 5.1; N, 1.5. Found: C, 54.8; H, 5.1; N, 1.6.

Spectral and analytical data for **2b**: ^{1}H NMR (δ, $CDCl_3$) 0.73 [s, 9H, $CNC(CH_3)_3$], 1.77 (m, 4H, 2 CH_2), 2.31 (m, 2H, CH_2), 2.53 (m, 2H, CH_2), 2.80−3.30 [m, 4H, $P(CH_2)_2P$], 7.42−7.96 (m, 20H, 2 PPh_2); $^{13}C\{^1H\}$ NMR (δ, $CDCl_3$) 24.5 (m, $PC_aH_2C_bH_2P$), 25.4 (s, CH_2), 26.0 (s, CH_2), 26.4 (m, $PC_aH_2C_bH_2P$), 28.9 (s, $CNC(CH_3)_3$), 32.8 (s, CH_2), 35.2 (s, CH_2), 58.2 [s, $CNC(CH_3)_3$], 127.9−133.3 (m, C_β, 2 PPh_2). Anal. Calcd for $C_{40}H_{42}BF_4NO_2P_2W$: C, 53.3; H, 4.7; N, 1.6. Found: C, 53.3; H, 5.1; N, 1.2.

Spectral and analytical data for **2c**: ^{1}H NMR (δ, $CDCl_3$) 0.75 [s, 9H, $CNC(CH_3)_3$], 1.55 (m, 6H, 3 CH_2), 1.78 (m, 2H, CH_2), 1.88 (m, 2H, CH_2), 2.18 (m, 2H, CH_2), 2.65 (m, 2H, CH_2), 2.80−3.30 [m, 4H, $P(CH_2)_2P$], 7.40−7.96 (m, 20H, 2 PPh_2); $^{13}C\{^1H\}$ NMR (δ, $CDCl_3$) 24.7 (m, $PC_aH_2C_bH_2P$), 25.4 (s, CH_2), 26.3 (s, CH_2), 26.6 (s, CH_2), 26.8 (m, $PC_aH_2C_bH_2P$), 27.1 (s, CH_2), 27.7 (s, CH_2), 29.1 (s, $CNC(CH_3)_3$), 32.7 (s, CH_2), 36.9 (s, CH_2), 58.3 [s, $CNC(CH_3)_3$], 128.2−133.6 (m, 2 PPh_2); MS (FAB, m/z) [$M^+ - BF_4$] = 856, [$M^+ - BF_4 - CO$] = 828, [$M^+ - BF_4 - CNC(CH_3)_3$] = 773. Anal. Calcd for $C_{43}H_{48}BF_4NO_2P_2W$: C, 54.7; H, 5.1; N, 1.5. Found: C, 55.2; H, 4.8; N, 1.2.

Spectral and analytical data for **2d**: ^{1}H NMR (δ, $CDCl_3$) 1.03 (m, 2H, CH_2), 1.23 (m, 8H, 4 CH_2), 1.74 (m, 4H, 2 CH_2), 2.27 (m, 2H, CH_2), 2.48 (m, 2H, CH_2), 2.80−3.30 [m, 5H, $CNCH(CH_2)_5$, $P(CH_2)_2P$], 7.40−7.87 (m, 20H, 2 PPh_2); $^{13}C\{^1H\}$ NMR (δ, $CDCl_3$) 22.3 (s, 2 CH_2), 24.1 (s, CH_2), 25.0 (m, $PC_aH_2C_bH_2P$), 25.4 (s, CH_2), 26.0 (s, CH_2), 26.9 (m, $PC_aH_2C_bH_2P$), 31.2 (s, 2 CH_2), 32.9 (s, CH_2), 35.2 (s, CH_2), 54.6 (s, $CNCH(CH_2)_5$), 128.5−133.6 (m, C_β, 2 PPh_2). Anal. Calcd for $C_{42}H_{44}BF_4NO_2P_2W$: C, 54.4; H, 4.8; N, 1.5. Found: C, 54.6; H, 4.9; N, 1.1.

Spectral and analytical data for **2e**: ^{1}H NMR (δ, $CDCl_3$) 1.03 (m, 2H, CH_2), 1.21 (m, 2H, CH_2), 1.78 (m, 6H, 3 CH_2), 1.51 (m, 8H, 4 CH_2), 1.75 (m, 2H, CH_2), 1.83 (m, 2H, CH_2), 2.17 (m, 2H, CH_2), 2.80−3.20 [m, 5H, $CNCH(CH_2)_5$, $P(CH_2)_2P$], 7.40−7.88 (m, 20H, 2 PPh_2); $^{13}C\{^1H\}$ NMR (δ, $CDCl_3$) 22.5 (s, 2 CH_2), 24.3 (s, CH_2), 25.0 (m, $PC_aH_2C_bH_2P$), 25.5 (s, CH_2), 26.4 (s, CH_2), 26.7 (s, CH_2), 27.0 (m, $PC_aH_2C_bH_2P$), 27.2 (s, CH_2), 27.7 (s, CH_2), 31.4 (s, CH_2), 32.8 (s, CH_2), 37.0 (s, CH_2), 54.8 [s, $CNCH$], 128.8−133.6 (m, 2 PPh_2); MS (FAB, m/z) [$M^+ - BF_4$] = 883, [$M^+ - BF_4 - CO$] = 855, [$M^+ - BF_4 - CNC_6H_{11}$] = 773. Anal. Calcd for $C_{45}H_{50}BF_4NO_2P_2W$: C, 55.8; H, 5.2; N, 1.4. Found: C, 55.3; H, 5.1; N, 1.5.

Spectral and analytical data for **2f**: ^{1}H NMR (δ, $CDCl_3$) 1.68 (m, 4H, 2 CH_2), 2.25 (m, 2H, CH_2), 2.40 (m, 2H, CH_2), 2.70−3.20 [m, 4H, $P(CH_2)_2P$], 4.32 (s, 2H, $CNCH_2Ph$), 6.60−7.75 (m, 25H, $CNCH_2Ph$, 2 PPh_2); $^{13}C\{^1H\}$ NMR (δ, $CDCl_3$) 25.4 (m, $PC_aH_2C_bH_2P$), 25.5 (s, CH_2), 26.1 (s, CH_2), 27.2 (m, $PC_aH_2C_bH_2P$), 32.9 (s, CH_2), 35.4 (s, CH_2), 47.9 (s, $CNCH_2Ph$), 126.8−133.7 (m, C_β, $CNCH_2Ph$, 2 PPh_2). Anal. Calcd for $C_{43}H_{40}BF_4NO_2P_2W$: C, 55.2; H, 4.3; N, 1.5. Found: C, 55.2; H, 4.3; N, 1.1.

Spectral and analytical data for **2g**: ^{1}H NMR (δ, $CDCl_3$) 1.45 (m, 6H, 3 CH_2), 1.72 (m, 4H, 2 CH_2), 2.14 (m, 2H, CH_2), 2.53 (m, 2H, CH_2), 2.80−3.20 [m, 4H, $P(CH_2)_2P$], 4.29 (s, 2H, $CNCH_2Ph$), 6.64−7.80 (m, 25H, $CNCH_2Ph$, 2 PPh_2); $^{13}C\{^1H\}$ NMR (δ, $CDCl_3$) 26.2 (s, CH_2), 26.5 (m, $PC_aH_2C_bH_2P$), 27.1 (s, CH_2), 27.4 (s, CH_2), 27.8 (s, CH_2), 27.8 (m, $PC_aH_2C_bH_2P$), 28.3 (s, CH_2), 33.4 (s, CH_2), 37.6 (s, CH_2), 48.6 (s, $CNCH_2Ph$), 127.5−134.4 (m, $CNCH_2Ph$, 2 PPh_2); MS (FAB, m/z) [$M^+ - BF_4$] = 890, [$M^+ - BF_4 - CO$] = 862, [$M^+ - BF_4 - CNCH_2Ph$] = 773. Anal. Calcd for $C_{46}H_{46}BF_4NO_2P_2W$: C, 56.5; H, 4.7; N, 1.4. Found: C, 56.8; H, 5.2; N, 1.6.

Spectral and analytical data for **2h**: ^{1}H NMR (δ, $CDCl_3$) 1.68 (m, 6H, 2 CH_3), 1.77 (m, 4H, 2 CH_2), 2.31 (m, 2H, CH_2), 2.60 (m, 2H, CH_2), 2.80−3.50 [m, 4H, $P(CH_2)_2P$], 6.91−7.90 (m, 23H, 2,6-$Me_2C_6H_3NC$, 2 PPh_2); $^{13}C\{^1H\}$ NMR (δ, $CDCl_3$) 17.7 (s, 2 CH_3), 25.5 (s, CH_2), 25.8 (m, $PC_aH_2C_bH_2P$), 26.1 (s, CH_2), 27.6 (m, $PC_aH_2C_bH_2P$), 33.2 (s, CH_2), 35.5 (s, CH_2), 125.5−135.5 (m, C_β, 2,6-$Me_2C_6H_3NC$, 2 PPh_2). Anal. Calcd for $C_{44}H_{42}BF_4NO_2P_2W$: C, 55.7; H, 4.5; N, 1.5. Found: C, 56.8; H, 5.2; N, 1.3.

Spectral and analytical data for **2i**: ^{1}H NMR (δ, $CDCl_3$) 1.51 (m, 6H, 3 CH_2), 1.67 (m, 6H, 2 CH_3), 1.75 (m, 2H, CH_2), 1.87 (m, 2H, CH_2), 2.20 (m, 2H, CH_2), 2.69 (m, 2H, CH_2), 2.80−3.40 (m, 4H, $P(CH_2)_2P$), 6.91−7.91 (m, 23H, 2,6-$Me_2C_6H_3NC$, 2 PPh_2); $^{13}C\{^1H\}$ NMR (δ, $CDCl_3$) 18.4 (s, 2 CH_3), 26.2 (s, CH_2), 27.0 (m, $PC_aH_2C_bH_2P$), 27.4 (s, CH_2), 27.5 (s, CH_2), 27.8 (s, CH_2), 28.3 (s, CH_2), 28.5 (m, $PC_aH_2C_bH_2P$), 33.7 (s, CH_2), 37.6 (s, CH_2), 126.3−135.7 (m, 2,6-$Me_2C_6H_3NC$, 2 PPh_2); MS (FAB, m/z) [$M^+ - BF_4$] = 904, [$M^+ - BF_4 - CO$] = 876, [$M^+ - BF_4 - (2,6\text{-}Me_2C_6H_3NC)$] = 773. Anal. Calcd for $C_{47}H_{48}BF_4NO_2P_2W$: C, 56.9; H, 4.9; N, 1.4. Found: C, 56.5; H, 4.6; N, 1.3.

Electrochemical Measurements

The electrochemical experiments were performed on an EG&G PARC 273 potentiostat/galvanostat connected to a PC computer through a GPIB interface (National Instruments PC-2A) or on an EG&G PAR 173 potentiostat/galvanostat and an EG&G PARC 175 Universal programmer. Cyclic voltammetry (CV) experiments were undertaken in a two-compartment three-electrode cell, at a platinum- or carbon-disk working electrode probed by a Luggin capillary connected to a silver wire pseudo reference electrode; a platinum auxiliary electrode was employed. Controlled potential electrolyses (CPE) were carried out in a two-compartment three-electrode cell with platinum-gauze working and counter electrodes in compartments separated by a glass frit; a Luggin capillary, probing the working electrode, was connected to a silver wire pseudo reference electrode. The electrochemical experiments were performed in a N_2 atmosphere at room temperature. The potentials were measured by CV in 0.2 mol dm^{-3} [NBu_4][BF_4]/CH_2Cl_2 or THF in the presence of ferrocene as the internal standard, and the values are quoted relative to the saturated calomel electrode (SCE) by using the $[Fe(\eta^5\text{-}C_5H_5)_2]^{0/+}$ redox couple ($E°$ = 0.53 or 0.55 V vs SCE, in CH_2Cl_2 or THF, respectively). The use, as reference electrode, of the SCE or other electrode in aqueous medium was avoided due to the sensitivity of the systems to water. The CPE experiments were monitored regularly by CV to ensure that no significant potential drift occurred along the electrolyses. The acid−base potentiometric titrations were carried out by using a standard solution of KOH in methanol. The results were corrected for background effects by performing also the titration of a blank solution of the electrolyte which has been electrolyzed under conditions identical to those used for the corresponding complex solution.

Computational Details

The full geometry optimization of model fragments was carried out in Cartesian coordinates using the quasi-Newton Raphson gradient method and the restricted Hartree−Fock

approximation with the help of the GAMESS program package.[28] The single-point electron correlation correction has been carried out for the equilibrium Hartree−Fock geometries at the second-order Møller−Plesset perturbation theory.[29] The symmetry operations were not applied. To take into account the relativistic effects for the core electrons of the W atom, the quasi-relativistic pseudopotential for 60 core electrons and the respective basis set for the tungsten atom[30] along with the analogous pseudopotentials and basis sets for other nonhydrogen atoms[31] have been used. The standard basis set of Gauss functions 6-31G[32] was selected for hydrogen atoms. Molecular orbital plots were generated using the program MOLDEN.[33]

The hypothetical complexes *trans*- and *cis*-$[(PH_3)_2(CO)_2(L)W(\equiv CCH{=}CH_2)]^{m+}$ [L = Cl^- (*m* = 0) ***trans*-1** or ***cis*-1**, NCMe (*m* = 1) ***trans*-2** or ***cis*-2**, CNMe (*m* = 1) ***trans*-3** or ***cis*-3**, or CO (*m* = 1) ***trans*-4** or ***cis*-4**] as well as *trans*- and *cis*-$[(H_2PCH_2CH_2PH_2)(CO)_2(L)W(\equiv CCH{=}CH_2)]^+$ (L = NCMe ***trans*-2′** or ***cis*-2′**, CNMe ***trans*-3′** or ***cis*-3′**, L = CO ***trans*-4′** or ***cis*-4′**) were chosen as model compounds for the corresponding complexes $[(dppe)(CO)_2(L)W\{\equiv CCH{=}\overline{CCH_2CH_2(CH_2)_nCH_2}\}]^{m+}$ (*n* = 1 or 4), and the known[2h] X-ray structure of *trans*-$[(dppe)(CO)_2(Cl)W(\equiv CCH{=}\overline{CCH_2CH_2CH_2CH_2})]$ was taken as the basis for the initial geometry of the calculated *trans*-isomers. The starting geometry of the *cis*-isomers was obtained by swapping L with one of the PH_3 ligands in the equilibrium *trans* isomeric structures.

Acknowledgment. This work has been funded by the DGICYT (Spain), the E.C. (Human Capital Mobility Programme; Project: ERBCHRXCT 940501), the Fundação para a Ciência e a Tecnologia (FCT) (Portugal), and the PRAXIS XXI Programme (Portugal). L.Z. acknowledges the financial support from the Spanish Ministerio de Educación y Ciencia (visiting researcher grant), the Agencia Española de Cooperación Internacional (Spain, doctoral fellowship), and the FCT (Portugal, postdoctoral PRAXIS XXI grant).

OM001095G

(28) Schmidt, M. W.; Baldridge, K. K.; Boatz, J. A.; Elbert, S. T.; Gordon, M. S.; Jensen, J. H.; Koseki, S.; Matsunaga, N.; Nguyen, K. A.; Su, S. J.; Windus, T. L.; Dupuis, M.; Montgomery, J. A. *J. Comput. Chem.* **1993**, *14*, 1347.

(29) (a) Møller, C.; Plesset, M. S. *Phys. Rev.* **1934**, *46*, 618. (b) Binkley, J. S.; Pople, J. A. *Int. J. Quantum Chem.* **1975**, *9*, 229.

(30) Andrae, D.; Haeussermann, U.; Dolg, M.; Stoll, H.; Preuss, H. *Theor. Chim. Acta* **1990**, *77*, 123.

(31) Bergner, A.; Dolg, M.; Kuechle, W.; Stoll, H.; Preuss, H. *Mol. Phys.* **1993**, *80*, 1431.

(32) Ditchfield, R.; Hehre, W. J.; Pople, J. A. *J. Chem. Phys.* **1971**, *54*, 724.

(33) Schaftenaar G.; Noordik, J. H. *J. Comput.-Aided Mol. Des.* **2000**, *14*, 123.